Weierstraß-Institut
für Angewandte Analysis und Stochastik

im Forschungsverbund Berlin e.V.

Preprint ISSN 0946 – 8633

Improving the stability of distributed-feedback tapered master-oscillator power-amplifiers

V.Z. Tronciu[1], M. Lichtner[1], M. Radziunas[1],

U. Bandelow [1] H.Wenzel [2]

submitted: 29th September 2009

[1] Weierstrass Institute
for Applied Analysis
and Stochastics,
Mohrenstrasse 39
D - 10117 Berlin
Germany
E-Mail:
tronciu@wias-berlin.de
lichtner@wias-berlin.de
radziunas@wias-berlin.de
bandelow@wias-berlin.de

[2] Ferdinand-Braun-Institut für
Höchstfrequenztechnik,
Gustav-Kirchhoff-Str. 4,
12489 Berlin, Germany
E-Mail: wenzel@fbh-berlin.de

No. 1444
Berlin 2009

2000 *Mathematics Subject Classification.* 35Q60, 35B30.

Key words and phrases. high power lasers, DFB MOPA, coupling coefficient, continuous wave.

1999 *Physics and Astronomy Classification Scheme.* 42.55.Px, 42.60.Pk, 42.60.Mi.

Edited by
Weierstraß-Institut für Angewandte Analysis und Stochastik (WIAS)
Mohrenstraße 39
10117 Berlin
Germany

Fax: + 49 30 2044975
E-Mail: preprint@wias-berlin.de
World Wide Web: http://www.wias-berlin.de/

Abstract

We report theoretical results on the wavelength stabilization in distributed-feedback master-oscillator power-amplifiers which are compact semiconductor laser devices capable of emitting a high brilliance beam at an optical power of several Watts. Based on a traveling wave equation model we calculate emitted optical power and spectral maps in dependence on the pump of the power amplifier. We show that a proper choice of the Bragg grating type and coupling coefficient allows to optimize the laser operation, such that for a wide range of injection currents the laser emits a high intensity continuous wave beam.

1 Introduction

During recent years, compact semiconductor lasers emitting single-frequency, diffraction limited continuous-wave (CW) beams at an optical power of several Watts have received considerable attention. Such lasers are required for many applications, e.g. frequency conversion [1, 2], laser display technology [3], and pumping of fiber lasers and amplifiers [4]. A device which is capable to maintain a good beam quality and wavelength stability in the Watt range is the monolithically integrated master-oscillator (MO) power-amplifier (PA), where either a distributed Bragg reflector (DBR) [5] or a distributed feedback (DFB) [6] laser and a flared (or tapered) gain-region amplifier are combined on a single chip. Several groups presented such high-power systems [7, 8] based on tapered laser devices [9] which promise a good beam quality and high output power at the same time. The narrow waveguiding MO part is responsible for the selection of a single lateral lasing mode, which is strongly amplified in the tapered PA part of the device. MOPA lasers are characterized by a large amount of structural and geometrical design parameters, and are subject to time-space instabilities like pulsations, self-focusing, filamentation and thermal lensing which yield restrictions to output power, beam quality and wavelength stability. In many cases changes in operating conditions (e.g. injection currents) of these devices imply destabilizations of the desired continuous wave (CW) beams with a consequent occurrence of various dynamical states. To simulate the dynamics of MOPA devices we apply a 2+1-dimensional partial differential equation model based on the traveling wave (TW) equations for the complex slowly varying envelopes of the counter-propagating optical fields: see Refs. [6, 10], where a good qualitative agreement between experiments and simulations is demonstrated.

In the present paper we consider the impact of the Bragg grating design on the dynamic performance of DFB MOPAs discussed in Refs. [6, 10] with respect to the

injection current in the PA part of the laser. We show that an increase of the coupling coefficient κ of a uniform Bragg grating allows to achieve stable CW emission without previously observed dynamic instabilities over a wide range of injection currents. We also show that an improved wavelength selectivity and stabilization can be realized by introducing a quarter-wavelength ($\lambda/4$) shift into the grating of the MO DFB laser.

The paper is organized as follows. The device structure and mathematical model are described in Section 2. Section 3 discusses the wavelength stabilization of the MOPA device by selecting different coupling coefficients and the Bragg grating type. Conclusions are given in Section 4.

2 Laser structure and mathematical model

A schematic representation of a DFB MOPA device is given in Fig. 1. It consists of an index-guided DFB ridge-waveguide laser and a gain-guided tapered amplifier combined on a single chip. Both facets are anti-reflection coated with a residual reflectivity of $R \approx 10^{-3}$. This small reflectivity at the front (PA) facet has been shown to generate multiple compound cavity modes. The latter give rise to mode transitions and possible dynamical instabilities when the injection currents into PA or MO are tuned [6, 10].

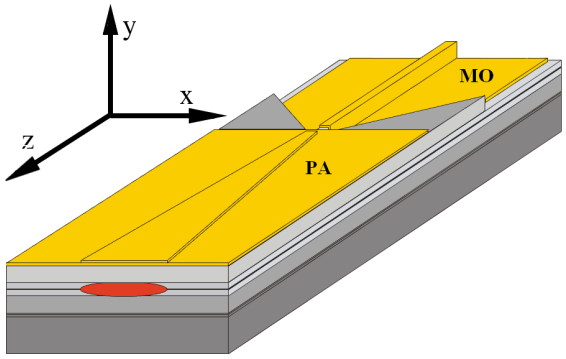

Figure 1: Scheme of a MOPA device consisting of a DFB Master Oscillator (MO) and a tapered Power Amplifier (PA). Both sections can be electrically individually pumped.

To simulate the dynamics of the MOPA device we use a traveling wave model [6, 11, 12] based on the 2+1-dimensional TW equations for the complex slowly varying amplitudes of the counter-propagating optical fields $u^{\pm}$:

$$\frac{1}{v_g}\partial_t u^{\pm} = \frac{-i}{2k_0\bar{n}}\partial_{xx}u^{\pm} + (\mp\partial_z - i\beta(z,x,N,J))\,u^{\pm} - i\kappa(z,x)u^{\mp} + F_{sp}^{\pm},$$

where t denotes time, while z and x correspond to longitudinal and lateral spatial directions (c.f. Fig. 1). v_g, $k_0 = 2\pi/\lambda_0$, $\overline{n}$, and $F_{sp}^{\pm}$ are the group velocity of light

inside the MOPA, the free-space central wavenumber inverse proportional to the central wavelength λ_0, the reference refractive index, and the spontaneous emission Langevine noise term, respectively. The complex propagation factor β is separately defined for different regions of the device and describes linear loss, gain, and refractive index in the semiconductor material. This factor depends on the excess carrier density N. Refractive index changes due to Joulean heating induced by injection currents are taken into account parametrically. The wavelength dependence of the gain is modeled by additional complex polarization equations which define a Lorentzian shaped gain spectrum. Finally, $\kappa = \kappa(z, x)$ is a complex field coupling parameter of the index-coupled DFB section. It is nonvanishing within the DFB MO part of the device and is zero elsewhere. For uniform gratings it is defined by some real positive constant, while for $\lambda/4$-shifted gratings it changes sign at the corresponding longitudinal position.

The remaining model equations for excess carrier density N, complex polarization functions, as well as a more detailed description of the factor β and other device parameters can be found in [6, 10]. We have solved the large scale system resulting from the numerical discretization of the model equations using high performance parallel distributed computing [13].

3 Wavelength stabilization

The Bragg-grating in the MO DFB part of the device, represented by κ, selects one or a few longitudinal modes corresponding to its main resonances. This is in contrast to Fabry-Perot (FP) type lasers ($\kappa = 0$), whose spectral selectivity is dominated by the wavelength-dependent gain function profile. Therefore, by increasing κ, one expects improved mode selection at the Bragg resonance with further suppression of all other compound cavity modes. Thus, we believe, mode transitions accompanied with dynamic instabilities observed in our previous study [6, 10] can be avoided by increasing κ.

To check these suggestions for DFB MOPA devices we have simulated the device described in [6] for successively higher values of the coupling coefficient κ in the DFB MO part of the laser. Panels a) and b) of Fig. 2 show field intensity and spectra for increasing PA current I_{PA} at four values of κ, starting from $\kappa = 250m^{-1}$ up to $\kappa = 3000m^{-1}$. A quick inspection of these figures shows that for $\kappa = 750m^{-1}$ and $\kappa > 1000m^{-1}$ the optical spectrum is stabilized and the dynamic instabilities disappear. Here the MOPA exhibits stable CW emission, but the output power is decreasing for larger κ. There exists an optimal range around $\kappa \sim 750m^{-1}$ where the output power is maximal while the device operates stably CW.

The slight redshift of the lasing wavelength with periodically occurring mode jumps for $\kappa = 250m^{-1}$ (see left side of Fig. 2b) was analyzed in our previous papers [6, 10]. For higher κ the neighboring longitudinal compound cavity modes are suppressed and the DFB MO becomes less sensitive to the optical feedback from the PA part

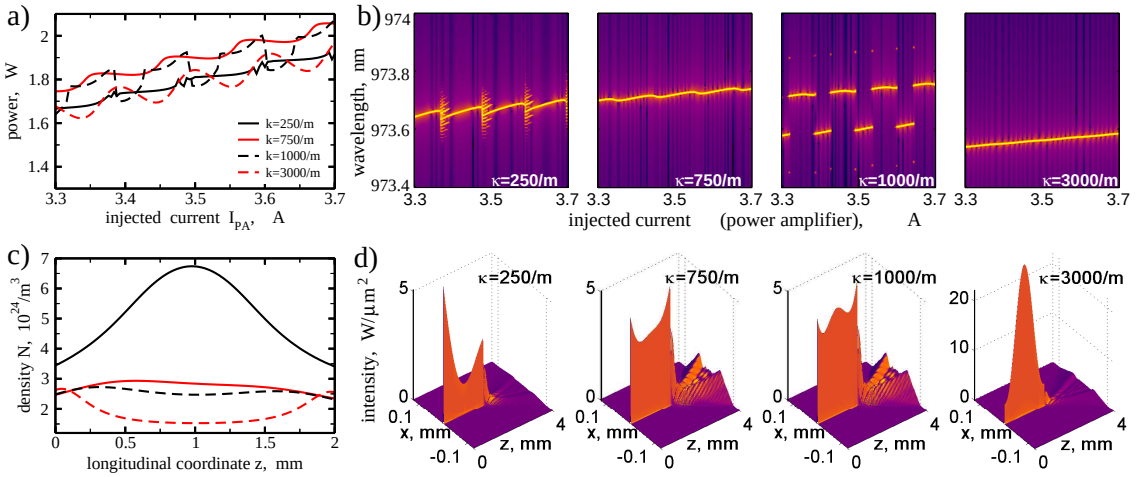

Figure 2: Simulations of DFB MOPA devices with uniform gratings for different values of κ. a),b): output intensity as a function of I_{PA} and corresponding mappings of the optical spectrum. c),d): longitudinal distribution of carrier density N within the DFB MO and corresponding total spatial field intensity distributions along the full computational domain at $I_{PA} = 3.7$A.

of the device, which occurs due to the residual field reflectivity at the PA facet. Consequently, the transitions and beatings between *neighboring* modes are no more observed. For $\kappa = 1000m^{-1}$, however, more distant DFB resonance modes get similar thresholds and periodic jumps between these modes occur. In this case, the dominance of a particular mode is sensitively decided by the phase difference of the complex fields u^+ and u^- at the interface of the MO and PA, which is tuned by the injected current [10]. The mechanism of transitions between two DFB resonance modes is, in general, similar to that one observed for $\kappa = 250m^{-1}$ (see left side of Fig. 2b) and discussed in [14]. Due to larger resonance mode separation for $\kappa = 1000m^{-1}$, however, the coupling between modes is weaker [15] and simultaneous operation of two modes can be observed only within tiny parameter intervals which are not resolved in our computations.

Panels c) and d) of Fig. 2 show typical distributions of carrier densities within the MO and photon densities within the full computational domain for different coupling coefficients κ. For small $\kappa = 250m^{-1}$ the coupling between the counter-propagating fields due to the Bragg grating is weak. Thus, a comparatively high gain, i.e. high values of carrier density N, is needed for lasing of the MO: see solid line in panel c) of Fig. 2. In this case the DFB MO can be interpreted as a FP-type waveguiding amplifier section: there is a nearly exponential amplification of the counter-propagating fields along the MO yielding photon density maxima at the ends of the MO (see the left part of Fig. 2d). In turn, the resulting longitudinal spatial hole burning (LSHB) depletes the carriers at the ends of the MO (see solid line of Fig. 2c). Increasing κ reduces the threshold gain and thereby the excess carrier density N (compare different lines in Fig. 2c) and in turn the LSHB. However, for large $\kappa = 3000m^{-1}$ the photon density concentrates in the middle of the MO (see

the right part of Fig. 2d). The resulting LSHB now depletes the carriers in the middle (see dashed-dotted line of Fig. 2c). While the carrier depletion at the edges of the MO observed at $\kappa \leq 750m^{-1}$ selects the red DFB stop-band side mode, the LSHB-induced depletion of carriers in the middle of the MO at larger κ selects the blue DFB stop-band side mode [16].

We note finally, that the mode jumping behavior shown for $\kappa = 1000m^{-1}$ in Fig. 2b) may also occur for larger or smaller values of κ depending on the relation between the Bragg wavelength and the material gain peak position [16]. For this reason a further optimization of the Bragg grating for single mode selection might be required.

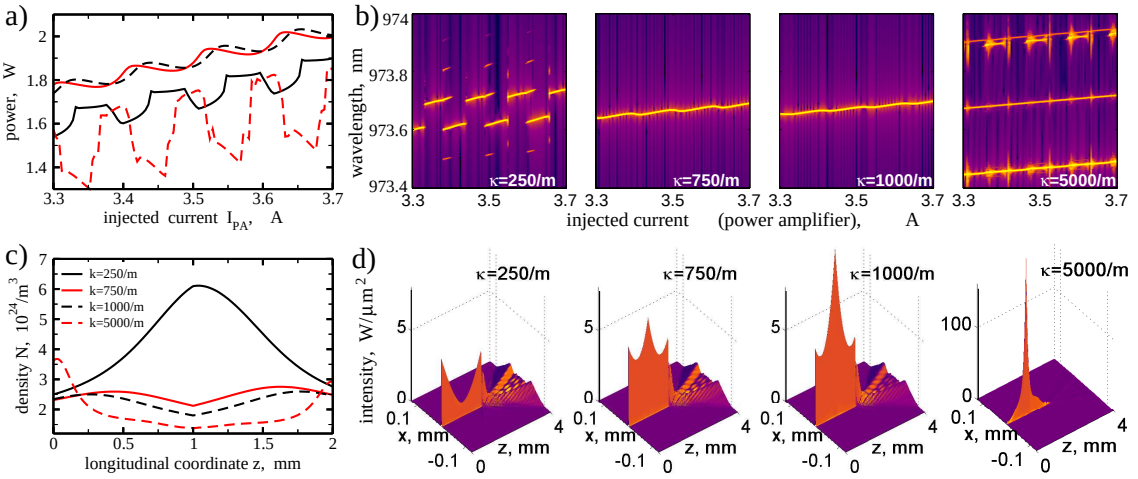

Figure 3: Simulations of DFB MOPA devices with $\lambda/4$-shifted gratings for different values of κ. The meaning of the panels is the same as in Fig. 2.

To avoid these stop-band mode transitions we finally propose to employ $\lambda/4$-shifted Bragg gratings, that support a single mode in the middle of the DFB stop-band and that are weakly sensitive to the optical feedback. Fig. 3 shows simulation results for $\lambda/4$ shifted DFB MOPAs with several values of κ. For smallest $\kappa = 250m^{-1}$ we observe again beatings and transitions between two modes. On the other hand, for large $\kappa = 5000m^{-1}$ the strong LSHB of carriers in the middle of the DFB MO supports the DFB stop-band side modes. At intermediate values of κ we find stable single-mode CW operation over the considered range of injection currents. However, the simulated output power decreases for larger coupling coefficients. An optimal coupling range providing stable single-mode CW operation with high output power could be found at about $\kappa = 750 - 1000m^{-1}$, which should be reasonably technologically accessible. Finally we mention that the results are basically independent of the phase of the back facet reflection.

4 Conclusions

Our previous theoretical and experimental study of MOPA devices emitting at 974nm [6, 10] has shown that tuning of the electrical pump into the MO or PA parts of the device implies periodic destabilizations of the desired CW states accompanied with regions of multimode operation as well as mode jumps to neighbouring CW states. In the present paper we have theoretically investigated the wavelength stability of DFB MOPA devices for different Bragg gratings. By increasing the coupling coefficient stable single mode CW operation over the full considered PA injection current range can be obtained. An additional improvement of mode selectivity with removed stop band side resonances can be achieved by introducing a $\lambda/4$-shift into the middle of the MO DFB grating. Both these optimizations of the grating design decrease the sensitivity of the MO DFB part of the device to the optical feedback induced by the residual PA facet reflectivity. As a consequence of the improved grating, the neighboring longitudinal compound cavity modes can not be excited by the residual optical feedback, such that the compound MOPA device stably operates on the same mode for all possible phases of the reinjected field. This yields in turn a nearly linear increase of the output power and of the wavelength with the PA injection current. The improved stability is accompanied with a slight output power drop-off at higher coupling values. Our simulations show that there exist optimal coupling ranges, where the MOPA exhibits stable single mode CW operation while a high output power is maintained.

We believe that our work provides a good basis for future studies, and, in particular, that it provides some pointers for more detailed investigations on stably operating high power lasers.

5 Acknowledgements

The work of M. Radziunas has been supported by DFG Research Center Matheon.

References

[1] C. Fiebig, G. Blume, M. Uebernickel, D. Feise, C. Kaspari, K. Paschke, J. Fricke, H. Wenzel, G. Erbert, "High-Power DBR-Tapered Laser at 980 nm for Single-Path Second Harmonic Generation", IEEE J. Select. Topics Quantum Electron., vol. 15, No. 3, pp. 978-983, 2009.

[2] O.B. Jensen, P.E. Andersen, B. Sumpf, K.-H. Hasler, G. Erbert, P.M. Petersen, "1.5 W green light generation by single-pass second harmonic generation of a single frequency tapered diode laser", Optics Express, vol. 17, no. 8, pp. 6532-6539, 2009.

[3] G. Hollemann, B. Braun, P. Heist, J. Symanowski, U. Krause, J. Kraenert, C. Deter, "High-power laser projection displays", Proc. SPIE, vol. 4294, pp. 36, 2001.

[4] A. M. Thomas, D. A. Alterman, M. S. Bowers, "High-peak-power Short Pulse Fiber Laser for Materials Processing", Proc. SPIE, vol. 7195, pp. 719518-1, 2009.

[5] H. Wenzel, K. Paschke, O. Brox, F. Bugge, J. Fricke, A. Ginolas, A. Knauer, P. Ressel, G. Erbert, "10W continuous-wave monolithically integrated master-oscillator power-amplifier", Electron. Lett., vol. 43, pp. 160-161, 2007.

[6] M. Spreemann, M. Lichtner, M. Radziunas, U. Bandelow, H. Wenzel, "Measurement and simulation of distributed- feedback tapered master-oscillator power-qmplifiers", IEEE J. Quantum Electron., vol. 45, no. 6, pp. 609-616, 2009.

[7] S. Schwertfeger, J. Wiedmann, B. Sumpf, A. Klehr, F. Dittmar, A. Knauer, G. Erbert, G. Tränkle, "7.4 W continuous-wave output power of master oscillator power amplifier system at 1083 nm", Electron. Lett., vol. 42, no. 6, pp. 346-347, 2006.

[8] M. Chi, O.B. Jensen, J. Holm, C. Pedersen, P.E. Andersen, G. Erbert, B. Sumpf, P.M. Petersen, "Tunable high-power narrow-linewidth semiconductor laser based on an external-cavity tapered amplifier", Opt. Express, vol. 13, no. 26, pp. 10589-10596, 2005.

[9] B. Sumpf, K.-H. Hasler, P. Adamiec, F. Bugge, F. Dittmar, J. Fricke, H. Wenzel, M. Zorn, G. Erbert, and G. Tränkle, "High-brightness quantum well tapered lasers" IEEE J. Select. Topics Quantum Electron., vol. 15, No. 3, pp. 1009-1020, 2009.

[10] M. Radziunas, V. Z. Tronciu, U. Bandelow, M. Lichtner, M. Spreemann, H. Wenzel, "Mode transitions in distributed-feedback tapered master-oscillator power-amplifier", to appear in Optical and Quantum Electronics, 2009.

[11] A. Egan, C. Z. Ning, J. V. Moloney, R. A. Indik, M. W. Wright, D. J. Bossert, J. G. McInerney, "Dynamic instabilities in master oscillator power amplifier semiconductor lasers", IEEE J. Quantum Electron., vol. 34, no. 1, pp. 166-170, 1998.

[12] S. Balsamo, F. Sartori, I. Montrosset, "Dynamic beam propagation method for flared semiconductor power amplifiers". IEEE J. Select. Topics Quantum Electron., vol. 2, no. 2, pp. 378-384, 1996.

[13] M. Lichtner, M. Spreemann, U. Bandelow, "Parallel simulation of high power semiconductor lasers", 9th International Workshop on State-of-the-Art in Scientific and Parallel Computing conference (Para 2008), to appear in LNCS

[14] V.Z.Tronciu, M. Lichtner, M. Radziunas, U. Bandelow, H. Wenzel, "Dynamics and stability improvement of DFB tapered master-oscillator power-amplifiers", Proceedings of the 6th International Conference on Microelectronics and Computer Science, Chisinau, Republic of Moldova, October 1-3, 2009.

[15] M. Radziunas, H.-J. Wünsche, "Multisection lasers: Longitudinal modes and their dynamics", in Optoelectronic Devices - Advanced Simulation and Analysis, pp. 121-150, ed. J. Piprek, Springer Verlag, New York, 2005.

[16] H.-J. Wünsche, M. Radziunas, S. Bauer, O. Brox, B. Sartorius, "Modeling of Mode Control and Noise in Self-Pulsating PhaseCOMB Lasers", IEEE J. Select. Topics Quantum Electron., vol. 9, no. 3, pp. 857-864, 2003.